Understanding clarification of sweet orange juice by microfiltration and fouling behaviour

Vishnuvardhan Sidlagatta[1*], Satyanarayana Veera Venkata Chilukuri[2], Smith Daniel Dasi[1], Bhaskararao Devana[1], Lakshmipathy Rangaswamy[3]

(1. Dr NTR College of Agricultural Engineering, Acharya NG Ranga Agricultural University, Bapatla, Indiar
2. Dr NTR College of Food Science & Technology, Acharya NG Ranga Agricultural University, Bapatla, India
3. Agricultural Research Station, Acharya NG Ranga Agricultural University, Amaravati, Andhra Pradesh, India)

Abstract: Sweet orange is an important citrus fruit grown throughout the world as it rich in phytonutrients properties and excellent source of vitamin C. The conventional clarification process involves more costs with personnel, equipment, and physical space. As an alternative, microfiltration (MF) has been applied in fruit juices for clarification. Clarification of sweet orange juice was carried out by microfiltration process using 0.2 μm size cellulose acetate MF membrane in a stirred cell. Flux decline was majorly due to deposits formed with soluble and suspended fraction of pectin, proteins and fibers, forming a low methoxy gel layer on membrane surface causing fouling during clarification. Long term flux decline was dictated by intermediate pore blocking in combination with growth of gel layer over the membrane surface. Reversible resistance was considered as domineering resistance and therefore, 90% of original permeate flux was recovered by following proper washing protocol to clean membranes. It was noticed that most of the total soluble solids (TSS), pH and vitamin C expressed as ascorbic acid of the feed were recovered in the permeate after filtration and there was no loss of the important properties pertaining to sweet orange juice.

Keywords: sweet orange, microfiltration, gel layer resistance, gel porosity

Citation: Vishnuvardhan, S., Ch. V. V. Satyanarayana, D. D. Smith, D. Bhaskararao and R. Lakshmipathy. 2023. Understanding clarification of sweet orange juice by microfiltration and fouling behaviour. Agricultural Engineering International: CIGR Journal, 25(2):222-234.

1 Introduction

Sweet orange (*Citrus sinensis*) is a predominant citrus fruit grown throughout the world as it rich in phytonutrients properties and excellent source of vitamin C. With multiple health benefits of vitamin C, there has been increased focus on research on development of value-added products of sweet orange juice in recent years. It is enjoyed most either as a juice or whole fruit. Unique feature of citrus juices is due to presence of juice sacs. A freshly squeezed sweet orange juice is an excellent thirst quencher and energizer. It will be much appreciated if the production of sweet orange juice after processing with better shelf life, closely emulates that raw fruit from which they are derived. The conventional clarification process involves many steps, such as depectinization (enzymatic treatment) (Machado et al., 2012), cooling, flocculation using gelatin and bentonite and diatomaceous earth (Pagliero et al., 2011; Bagci, 2014), centrifugation (Chhaya et al., 2013), decantation,

Received date: 2022-04-25 **Accepted date:** 2022-12-11

* **Corresponding author: S. Vishnuvardhan,** Associate Professor, Department of Processing and Food Engineering, Dr. NTR College of Agricultural Engineering, Acharya N.G. Ranga Agricultural University, Bapatla – 522 101, Andhra Pradesh, India. Email: vishnuvardhans@angrau.ac.in. Tel: +91-9440363112.

and filtration (Sagu et al., 2014), requiring more costs with personnel, equipment, and physical space (Rai et al., 2006). The ultrafiltration (UF) and microfiltration (MF) have been applied in fruit juices and pulps and wines industries, reducing many steps of the conventional clarification (Razi et al., 2011).

MF separates the molecules according to size or molecular weight cutoff (MWCO) of the membrane, producing a permeate and a retentate. In this process, large molecules (e.g. fat globules) and suspended particles are held by the membrane while the dissolved components pass through the membrane. MF resembles conventional coarse filtration and can selectively separate particles of size 0.1 to 10 microns, mostly macromolecules by utilizing membranes with the pore sizes ranging from 0.05-10 μm at an applied pressure of 0.1-2.0 bar. Applications of microfiltration include fruit juice clarification, casein and whey protein separation, oil-water emulsions separation and wastewater treatment (Kotsanopoulos and Arvanitoyannis, 2015) with the clear advantages of low energy consumption and simpler process. Other major advantages offered by MF process in comparison to the conventional process is that flexibility in operating at moderate temperatures with shorter processing time. Further, in the conventional process, the major limitation is the usage of filter aids which are costly and pose environmental concern during disposal (Habibi et al., 2011). The demand on industry for environment friendly and cleaner technology is also driving fruit juices clarification using membrane technology. Clarifications of several fruit juices *viz*., banana (Sagu et al., 2014), tomato (Razi et al., 2011) carrot (Habibi et al., 2011), water melon (Rai et al., 2010), Pomegranate (Mirsaeedghazi, et al., 2011), orange (Cassano et al., 2009), cashew apple (Wolkoff et al., 2004), pineapple (Carneiro et al., 2002) through microfiltration were reported. The major practical limitation of microfiltration is the reduction of permeate flux with time due to fouling that reduces the competitiveness of the process in comparison to the conventional process (Rai et al., 2006; Rai et al., 2010; Cassano et al., 2009). It is important to understand the reasons behind flux decline and to analyze mechanisms of various membrane pore blocking through available models. Further, few researchers analyzed the phenomenon of flux decline using resistance in series model (Pagliero et al., 2011; Brião and Tavares, 2012) considering intrinsic membrane resistance, reversible fouling resistance and irreversible fouling resistance that play a major role in determining whether adhesion of solutes occurs preferably in the external region (ie., higher reversible resistance) or inner pores of membranes (irreversible fouling resistance). The knowledge on type of fouling resistance infers the clue on the steps to be taken so as to recover the permeate flux.

Thus, in this study, an attempt has been made to identify the permeate flux decline mechanism during microfiltration of sweet orange juice based on Hérmia's theory (1982) and the data was analysed using an available models (Field et al., 1995; Wu, 2021). Further, fouling behaviour of MF membrane was investigated during microfiltration of sweet orange juice using circuit of resistors connected in series analogy to assess whether major adhesion takes place externally over membrane surface or internally within pores for recovery of the permeate flux.

2 Materials and methods

2.1 Raw material preparation

Freshly harvested matured sweet orange fruits (Variety: *Sathgudi*) with a maturity index of colour change from green to pale green with shiny and oil glands on rind (acidity 0.3%, total soluble solids[TSS]: 9-10 °Brix) were procured from local market. Adhering dust to fruits were cleaned with water and shade dried to remove surface moisture. For determining juice properties, various preparatory activities included cutting, juice extraction using press type hand operated sweet orange juice extractor (Basant), pre-filtration using muslin cloth, addition of sodium benzoate @ 0.1% as a

preservative (Shahnawaz et al., 2013) were carried out.

Microfiltration clarification experiments on sweet orange juice were carried out in a batch mode using stirred cell set up. The cell had three detachable parts viz., top flange, middle cylindrical feed cell and bottom stainless steel support with grooved based for holding the circular membrane having an effective filter area of 33.16 cm^2. The top flange was housed with stirrer powered by a motor through a belt. Middle cylindrical shell has a capacity of 500 mL connected to a nitrogen cylinder to generate required transmembrane pressure. Juice was fed manually to cell made of stainless steel with a capacity of 500 mL. The stirrer speed was measured by hand held digital tachometer. Stirrer speed was maintained using a variac at an rpm of 1500±100. MF experiments using cellulose acetate membrane (pore diameter of 0.2 μm) were carried out at a transmembrane pressure of 68.9, 137.89 and 206.84 kPa (10, 20 and 30 psi, respectively). The slope of flux data versus pressure curve gave the permeability of the membrane.

Initially compaction of membranes was carried out at a pressure of 275.8 kPa (40 psi) using distilled water for duration of 2 hours. The pure water flux through microfiltration membrane was determined by charging the cell with 300 mL distilled water. All clarification experiments were conducted at the room temperature of 30 ±2 °C. After water run, the cell was charged with 200 mL of pre-filtered juice and was subjected at the operating pressure using a pressure regulator of a nitrogen cylinder. Permeate from the bottom of cell was collected at an interval of 10 min in a beaker and cumulative volume was noted.

The duration of each experiment was about 60-90 min. After the experiment the set up was dismantled and the weight of the membrane before and after experiment before washing was recorded for analysis of membrane resistance. The feed cell and membrane were washed thoroughly using distilled water after each experiment. Further, distilled water was used to rinse the membrane carefully without rubbing on its surface. Subsequently, on through washing, a water run was taken again to measure the change in the permeability. On variation of permeability by ±5% for successive runs, washing was done with 0.5 N HCl followed by 0.1 N NaOH and then final washing with distilled water as per protocol of the manufacturer. At the end of the experiment, the permeate sample was collected and analyzed. Further, a plot of cumulative volume versus time was drawn. Various dependent variables that were measured include: permeate flux (L $h^{-1}m^{-2}$), TSS (Atago make Handheld Refractometer, 0-52 °Brix, model PAL-1), pH (Eco tester pH1 meter); viscosity (Brookfield viscometer, model: DV1MLV), colour in terms of per cent absorbance at 420 nm (Rayleigh make UV-Vis Spectrophotometer) and clarity in terms of per cent transmittance at 420 nm (Rayleigh make UV-Vis Spectrophotometer).

2.2 Identification of fouling mechanism

The analysis of the characteristics curves was carried out to determine mode of permeate flux decline during filtration (Hérmia, 1982; Kyo-Jen et al., 2003).

$$\frac{d^2t}{dV^2} = k\left\{\frac{d^2t}{dV^2}\right\} \quad (1)$$

where, t (s) is the cumulative time of the instantaneous cumulative volume (V, mL), and k and n are the parameter constants. For different modes of microfiltration, n assumes different values. It is 2.0 for complete blocking, 1.5 for standard blocking, 1.0 for intermediate blocking, and 0 for cake filtration (Table 1).

In the above table, a plot of $\frac{1}{J^2}$, $\frac{1}{J}$, $\frac{1}{\sqrt{J}}$ and $ln(\frac{1}{J})$ with t individually, is a straight line, then existent predominant mechanism was considered to be cake formation, intermediate blockage, standard and complete blockage, respectively.

2.3 Estimation of specific gel layer resistance

Permeate flux (J) is determined as per classical equation for flow through dead-end filter using Darcy's law using the total resistance offered by the membrane (R_m) and the gel layer (R_g).

$$J = \boldsymbol{\Delta V}/(A_m \times \Delta T) = \Delta p/(\mu \times (R_m + R_g)) \quad (2)$$

where, ΔV is the permeate volume collected (mL), A_m is the effective area of membrane, 0.0034 m^2, ΔT is the time to collect the permeate volume (s), R_m is the clean membrane resistance (m^{-1}) and R_g is the resistant due to gel layer during arbitrary transient time (m^{-1});

Δp is the transmembrane pressure (kPa);

μ is the viscosity of the solution (mPa.s).

Above Equation 2 was linearized and R_g was re-written in terms of specific gel layer (α) resistance, gel porosity (ε_g), density of gel (ρ_g) as

$$\frac{1}{J^2} = \frac{1}{J_o^2} + 2\alpha C_b \mu/\Delta p = \frac{1}{J_o^2} + \phi \times t \qquad (3)$$

$$\phi = 2\alpha C_b \mu/\Delta P \qquad (4)$$

where, $\boldsymbol{\mu}$ is the viscosity of feed solution (mPa s), C_b is the weight of the gel collected over membrane surface (kg m^{-3}). ϕ =slope parameter obtained from the plot between $\frac{1}{J^2}$ and t (m^4 h/L^2)

The Equation 3 was in the form of Y = mx + C with slope m and intercept C. By plotting $\frac{1}{J^2}$ versus t gives the value of slope ϕ and on substitution in Equation 3, the value of $\boldsymbol{\alpha}$ was obtained.

Table 1 Solutions of Equation 1 for different values of *n*

Fouling mechanisms	n	Fouling models	Linear form	Straight line plot
Cake filtration	0	$J = J_o/(1+J_o^2kt)^{0.5}$	$\frac{1}{J^2} = (1/J_o^2) + kt$	$\frac{1}{J^2}$ *vs. t*
Intermediate blockage	1	$J = J_o/(1+J_okt)$	$\frac{1}{J} = (1/J_o) + kt$	$\frac{1}{J}$ *vs. t*
Standard blockage	1.5	$J = J_o/(1+J_o^{0.5}kt)^2$	$\frac{1}{\sqrt{J}} = (1/J_o^{0.5}) + kt$	$\frac{1}{\sqrt{J}}$ *vs. t*
Complete blockage	2	$J = J_o exp(-kt)$	$ln(\frac{1}{J}) = ln(1/J_o) + kt$	$ln(\frac{1}{J})$ *vs. t*

Note: k= parameter related to solute property; J_o is the initial flux

2.4 Evaluation of compressibility of filter cake

Specific cake resistance (α) is dependent on void fraction (ε), ratio of specific surface area to volume of solid particle (S_o) and transmembranepressure (TMP, ΔP). By conducting experiments at varying TMPs, the change in α with Δp was determined (Zaidi and Kumar, 2005).

$$\alpha = \alpha_o (\Delta P)^n \qquad (5)$$

where, α_o and n are empirical constants and 'n' is the compressibility constant.

Linearized form of Equation 5 was obtained by applying logarithm on both sides as

$$ln(\alpha) = ln(\alpha_o) + n\, ln(\Delta P) \qquad (6)$$

On plotting $ln(\alpha)$ values with $ln(\Delta P)$, which takes linear form with slope as 'n' and intercept as $ln(\alpha_o)$ values. If α is independent of (ΔP), the cake is incompressible (where, n=0).

2.5 Determination of gel porosity

The average size of the solid particles in gel layer (d_p) was estimated considering the spherical molecules and using an empirical equation as per Stryer (1998).

$$M_w = z d_p^3 \qquad (7)$$

where, M_w is average molecular weight of gel forming layer (kDa), z is empirical constant. The gel porosity (ε_g, ratio) was calculated from Kozeny-Carman equation (Rai et al., 2005) at a particular pressure using iterative procedure assuming that gel characteristics to be same as gel.

$$\alpha = 180\,(1-\varepsilon_g)/\varepsilon_g\, d_p^2 \rho_g \qquad (8)$$

2.6 Interpretation of fouling by resistance measurements

Steady state permeate juice flux through porous membrane written in terms of TMP, total membrane resistance (R_t), permeate viscosity (η) as:

$$J = \frac{\Delta P}{\eta R_t} \Rightarrow R_t = \frac{\Delta P}{\eta J} \qquad (9)$$

The R_t was interpreted as summation of the resistances due to configuration and built of membrane itself (R_m, intrinsic membrane resistance); resistance due to concentration polarization (R_r, reversible resistance); and resistance due to internal/partial/complete pore blocking causing irreversible fouling (R_i, irreversible

fouling resistance).

$$R_t = R_m + R_r + R_i \quad (10)$$

Pure water flux (J_w) through the new membrane was obtained experimentally and intrinsic membrane resistance (R_m) was calculated as:

$$J_w = \frac{\Delta P}{\eta_w R_m} \Rightarrow R_m = \frac{\Delta P}{\eta_w J_w} = \frac{1}{\eta_w L_h} \quad (11)$$

where η_w and L_h is the pure water viscosity (mPa.s) and hydraulic permeability (m^3 m^{-2} s^{-1} Ъa^{-1}).

Irreversible fouling resistance was calculating by removing reversible resistance barriers from the fouled membrane with pure water wash and then pure water flux (J_i) was estimated:

$$J_i = \frac{\Delta P}{\eta_w (R_i + R_m)} \Rightarrow R_i = \frac{\Delta P}{\eta_w J_i} - R_m \quad (12)$$

Reversible resistance was obtained as (Equation 13)

$$R_r = R_t - R_m - R_i \quad (13)$$

2.7 Physico-chemical properties

Hand held pocket Refractometer (Make: Atago, Model: PAL-1, Range:0-53 ЪBrix, Accuracy: ±0.2 ЪBrix, with automatic temperature compensation) was used to find total soluble solids of the juice. Aliquot of sample (~3 drops i.e., 0.3 mL) was fed to the refractometer prism, avoiding bubbles and large pulp particles (Amador, 2011) and the value displayed was noted. The pH measurement was performed using a digital pH meter (Eco Tester pH1). The glass electrode of the device was placed inside the homogenized sample of juice and the value was noted.

UV-Vis Spectrophotometer (Rayleigh) was used to measure clarity and colour of the feed/permeate (Amador, 2011; Rai et al., 2010). For measuring clarity and colour, the colorimeter was set to 100% light transmission at 650 nm and 100% light absorbance at 420 nm, respectively against distilled water in a cuvet. Test tube cuvet was decanted and filled with juice sample to be measured.

2.8 Estimation of ascorbic acid content

Ascorbic acid in the sample was determined as per procedure suggested by Ranganna (2010).

3 Results and discussion

The permeability of membrane (0.2 μm) membrane was estimated to be 5.095 L m^2 ћ kPa (1.415×10^{-8} m^3 m^{-2} s^{-1} Ъa^{-1}).

3.1 Influence of transmembrane pressure on permeate flux during MF of sweet orange juice

MF clarification of pre-filtered juice was done at three TMPs at 68.94, 137.89 and 206.84 kPa each replicated three times and graph between permeate flux and TMP was established (Figure 1). Initial juice flux was reduced by 18-20 times of pure water flux at the same transmembrane pressures. Initial permeate flux at TMP 68.94 kPa was 97.06 L m^{-2} h^{-1} and declined to steady state flux of 26.47 L m^{-2} h^{-1}. Similarly, initial and steady state permeate flux at TMPs 137.89 and 206.89 kPa, respectively were recorded as 118.23 and 141.18 L m^{-2} h^{-1} and 31.765 and 37.06 L m^{-2} h^{-1} .

The performance of filtration membrane can be assessed with the motif of flux reduction during operational time. There was a rapid and swift decline in flux during initial stage and slow and steady decline at later stages. Swift decline mighty be majorly due to deposits of left over pectin and higher molecular weight proteins, cellulose and hemicelluloses causing growth of polarized gel layer on the membrane surface. Similar trend of flux reduction for clarification using MF were reported by Carneiro et al. (2002) for pineapple juice; Habibi et al. (2011) for carrot juice; Rai et al. (2010) for watermelon juice; Razi et al. (2011) for tomato juice; Pagliero et al. (2011) for orange juice and Kazemi et al. (2013) for beer.

This decrease might be due to plugging of membrane pores and deposition on membrane surface by insoluble proteins, pectins, amino acids and phosphatides that are abundantly found in juice vesicles, albedo, flavedo and seeds (Kale and Adsule, 1995). Further, literature suggested that divalent calcium ions were found in abundance (100 mg kg^{-1}) in orange juice of 11.8 ЪBrix

(Syed et al., 2012). Further, an array of calcium ions has been reported to get crossed linked with pectins having 50 per cent degree of esterification forming an arrangement similar to egg box, thus, a low methoxy gel was formed that can liquefy its structure either thermally and/ or by mechanical agitation and reverses on subsiding of heat or agitation (Philip and Davis, 1992). Further, particle size distribution in orange juices was analyzed and reported by Buslig and Carter (1974) and Corrideg et al. (2001). Typical values of average particle volume (expressed as 10^{-5} µm^3 mL^{-1} juice) for different particle sizes for hard squeezed juice were reported as 1-2 µm (38.00), 2.0-6.35 µm (64.30), 16-64 µm (8.15) and 256-1024 µm (3.02) clearly indicating that 72% of particles in juice has size more than 2 µm and hence retained and gel formed on the membrane. Further, dissolved and suspended proteins, fibre and pectins might contribute for fouling over membrane surface and thereby causing decline of flux.

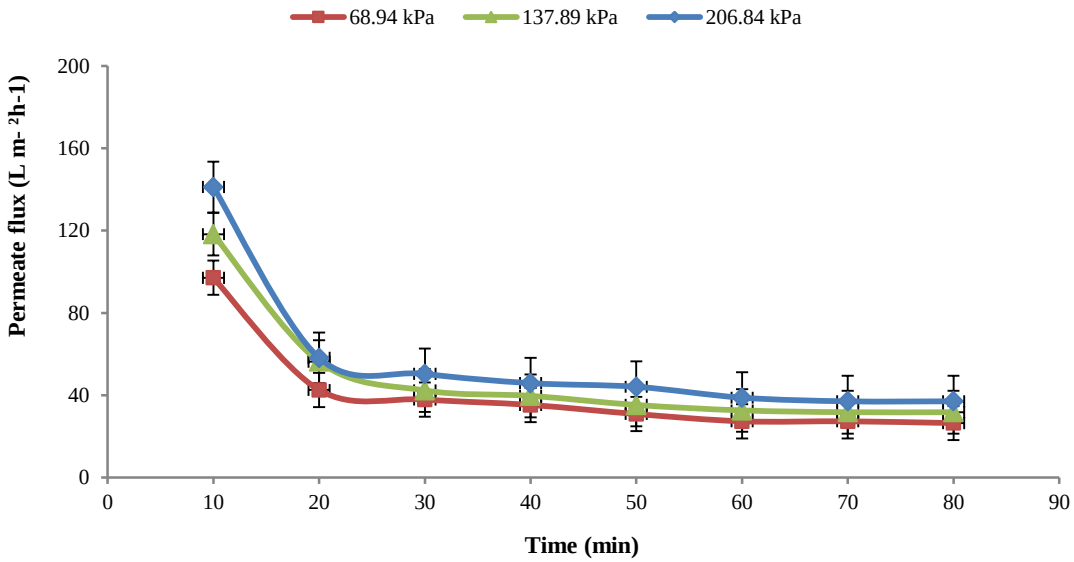

Figure 1 Flux decline during MF of sweet orange juice using 0.2 µm cellulose acetate membrane

Further, as TMP increased from 68.94 to 206.84 kPa, initial as well as steady state flux increased. Commonly, the permeate flux is enhanced with TMP. However, at certain limiting value of TMP, flux becomes independent of TMP as concentration polarization layer is induced by mass transfer region rather than pressure controlled region. Lei et al. (2016) and Kirk et al. (1983) reported that at higher TMP beyond critical flux, pectic gel layer was compressed, molecular bridges get collapsed leading to narrowing or closure of interstitial spaces between pectic chains, thus, eventually decreases permeate flux. Literature on gel layer and pressure independent region have been reported (Nakamura and Matsumoto, 2013). However, in the present experiment, permeate flux was fully regulated by pressure dominated region in the operating pressure range, indicating that limiting flux was not reached.

3.2 Identification of fouling mechanism

The obtained flux data was fitted to linear forms of the empirical models to find pattern of flux reduction due to either formation of internal fouling or gel layer (Figure 2 and Table 2). Inadequate fit of data with poor coefficient of determination suggested that mechanism of complete or standard pore blockage might not be the reason for fouling. Gel layer formation might be the prime factor for flux decline during MF clarification. Further, intermediate pore blocking might be contributing to the fouling during initial periods of filtration. Several researchers followed similar analogy to identify flux declining as well as fouling mechanism and reported internal pore blocking mechanism for chitosan (Domingues et al., 2014); complete pore blocking for

beer (Kazemi et al., 2013); cake filtration for passion fruit juice (Oliveira et al., 2012); cake or gel filtration for orange juice (Nandi et al., 2012); gel or cake filtration for watermelon (Rai et al., 2010).

Table 2 Statistical parameters for fitting of the characteristic equations with experimental data of Microfiltration of sweet orange juice

TMP (kPa)	Sum of squares (SS)				Error Mean sum of square (MSE)			
	Gel	CPB	IPB	SPB	Gel	CPB	IPB	SPB
68.9	1.46×10^{-6}	0.969	4.64×10^{-4}	0.005	1.2×10^{-8}	0.055	1.04×10^{-5}	2.04×10^{-4}
137.89	7.51×10^{-7}	1.023	3.62×10^{-4}	0.004	9.5×10^{-9}	0.065	8.97×10^{-6}	2.13×10^{-4}
206.84	3.78×10^{-7}	0.965	2.37×10^{-4}	0.002	3.8×10^{-9}	0.067	6.73×10^{-6}	1.79×10^{-4}
	Adj R^2				Std Error			
	0.945	0.701	0.878	0.787	1.09E-4	0.235	0.003	0.014
	0.917	0.676	0.867	0.756	9.77E-5	0.255	0.002	0.014
	0.933	0.654	0.850	0.872	6.18E-5	0.260	0.002	0.049

Note: Gel - Gel formation; CPB - Complete pore blocking; IPB - Intermediate Pore blocking; SPB – Standard pore blocking

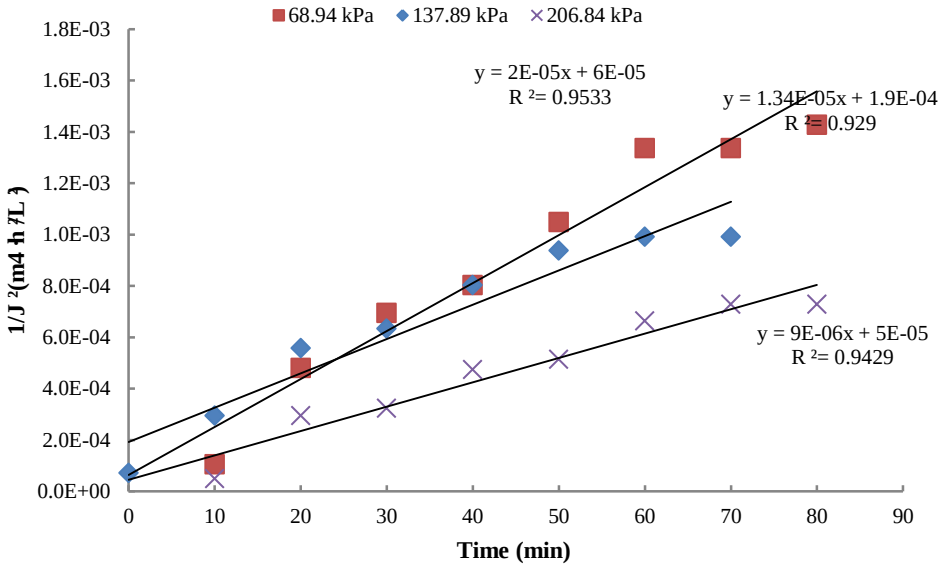

(a) Gel filtration

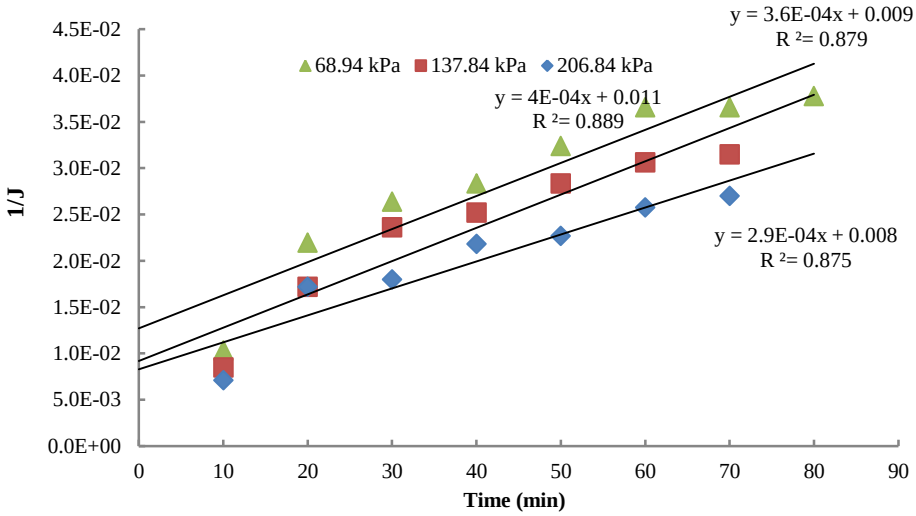

(b) Intermediate pore blockage

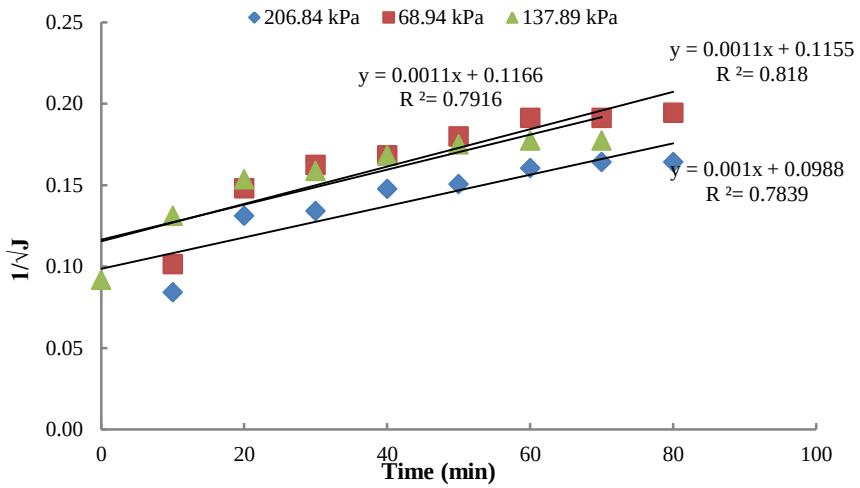

(c) Standard pore blockage

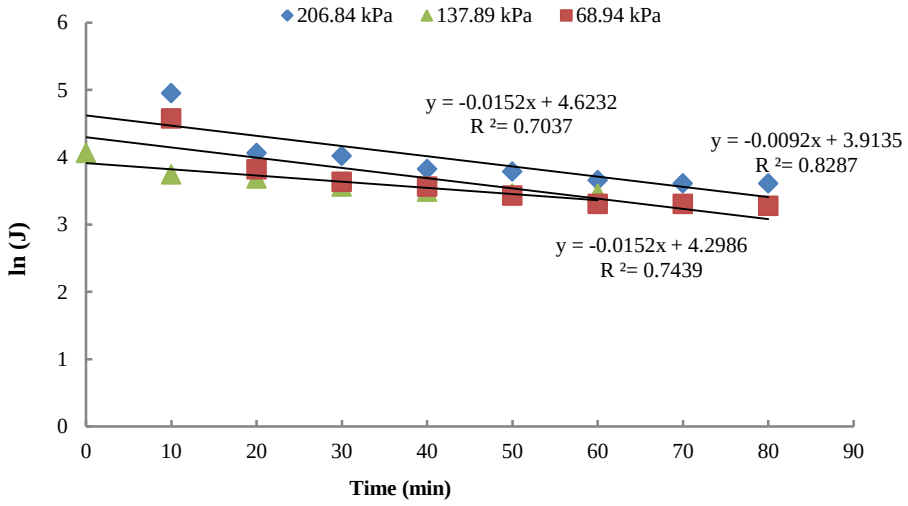

(d) Complete pore blockage

Figure 2 Fouling models of MF of sweet orange juice in a stirred cell

3.3 Estimation of specific gel layer resistance

The plot $1/J^2$ versus time data resulted in straight line (Figure 2a) with slope of the curve indicating the value of specific gel layer resistance. The slopes (ϕ) of the trend line for 206.84, 137.89 and 68.94 kPa were calculated to be 9×10^{-6}, 1×10^{-5} and 2×10^{-5}, respectively. Substituting the value ϕ in Equation 4 at different TMP's and substituting other parameters like μ, C_b and Δp, the value of α was observed. The value of C_b was directly measured at the end of the experiment with solids and other heavy molecular weight and left over pectin on the membrane surface and the specific gel resistance were estimated (Table 3). It was found that there is a direct correlation between TMP and specific cake resistance as former increased from 68.94 to 206.84 kPa, the later also increased from 2.493×10^{15} to 5.192×10^{15} (m kg^{-1}).

3.4 Determination of gel compressibility constant (*n*)

The empirical constants α_o and n were obtained from exponential of intercept and exponential of slope of the fitted linear plot between $ln(\alpha)$ and $ln(\Delta p)$. Gel compressibility constant (n) was determined as 0.706. Since, gel compressibility value of '0' was considered as incompressible and '1' as highly compressible, the gel compressibility constant in case of MF obtained might be specified as medium compressible. The determined values were as stated in Table 4.

Table 3 Computed values of Specific gel layer resistance (m kg^{-1}) and gel porosity during MF of sweet orange juice at various TMPs

Transmembrane pressure (Δp, kPa)	Computed Specific gel resistance (α, m kg^{-1})	Gel porosity (ε)
68.94	2.483×10^{15}	0.650
137.89	5.072×10^{15}	0.555
206.84	5.192×10^{15}	0.552

Table 4 Computation of gel compressibility constant

Parameter	Values obtained from graph	Exponential of values
α_o	27.63	9.989×10^{11} m kg^{-1}
Gel compressibility constant (n)	0.706	-

3.5 Determination of gel porosity

Considering organic nature of low methoxy gel formed by pectin with divalent calcium ions, Stryer (1998) proposed z as 6×10^{29} g mol m^{-3}. Further, substituting average global molecular weight of pectin as 100 kDa (Hoagland et al., 1997; Rai et al., 2006), size of a gel forming pectin particle was approximated as 5.5 nm.

The gel porosity (ε) was obtained at a particular TMP using iterative procedure using Kozeny-Carman equation assuming that gel characteristics to be same as gel as per Equation 8 (Oers et al., 1992; Zaidi and Kumar, 2005). The average gel density over membrane was approximated to be 3054 kg m^{-3} for all the experiments. In iterative method, gel porosity (ε) was first assumed and then gel resistance was computed and checked with estimated value. Iterations were continued till specific gel resistance values estimated and computed values were same and gel porosity values were presented (Table 3). The gel porosity values varied from 0.650 to 0.552 as TMP increased from 68.94 to 206.89 kPa. As TMP increased, the gel porosity values decreased as gel layer was more compacted leaving a little molecular space comparatively.

3.6 Interpretation of membrane and fouling resistances

3.6.1 Intrinsic membrane hydraulic resistance (R_m)

The hydraulic permeability of membrane was determined at 28±2 ℃ as L_h=1.368 × 10^{-9} m^3 m^{-2} s Pa or 499.2 L m^{-2} h bar. Intrinsic membrane resistance, R_m was calculated as 9.124 x 10^{11} m^{-1}. Pagliero et al. (2011) identified that the hydraulic permeability of the PVDF-PMMA MF membrane as 1195 L m^{-2} h^{-1} bar and intrinsic membrane resistance as R_m=3.01 x 10^{12} m^{-1}. Difference in the intrinsic membrane resistance might be the result of difference in material composition of the membranes.

3.6.2 Membrane total resistance (R_t)

The membrane total resistance, R_t was interpreted as sum of contributing resistances- in-series model. Steady state flux was considered while computing membrane total resistance (Table 5).

Irreversible fouling resistance was obtained by following Equation 12. It was observed that irreversible membrane resistance increased from 1.619×10^{11} to 3.20×10^{11} m^{-1} with increase in transmembrane pressure. Finally, reversible resistance was computed using Equation 13.

It is important to know that the ratio of resistance (R_m/R_t ; R_i/R_t and R_r/R_t) at different TMPs (Table 5) furnish greater insight to understand to what extent original permeate fluxes were achieved after cleaning process (Youn et al., 2004).

The main dominating resistance on the whole range of operating transmembrane pressures was studied. Reversible resistance was considered as domineering resistance (91.96% to 95.25%). The intrinsic membrane resistance was ranged between 2.70%-5.79% and

irreversible resistance was contributing to 2.05%-2.25% of the total resistances. Further, around 90% original permeate flux was recovered by following proper washing to clean the MF membranes.

The effect of TMP on membrane resistances showed that the total and reversible resistances had significant increase as Δp increased and irreversible resistance was almost constant. This phenomenon could be explained by assuming that an increase in TMP increases more settlement of solute particles on membrane due to increase in convenctive flux of the juice. Further, contributing to enhanced concentration polarization and gel layer thickness which in turn increased total and reversible resistance (Cassano et al., 2009). Similar high proportion of reversible resistance was reported by Pagliero et al. (2011) for orange juice and Chilukuri et al. (2001) for lactoferrin solutions during MF.

Table 5 Estimated values of membrane total (R_t), irreversible (R_i) and reversible resistances (R_r) and resistance ratios at various TMPs

Transmembrane pressure (Δp), kPa	R_t (m^{-1})	R_i (m^{-1})	R_r (m^{-1})	R_m/R_t (%)	R_i/R_t (%)	R_r/R_t (%)
68.94	7.19×10^{12}	1.62×10^{11}	6.61×10^{12}	5.79	2.25	91.96
137.89	1.19×10^{13}	2.56×10^{11}	1.13×10^{13}	3.47	2.13	94.39
206.84	1.54×10^{13}	3.20×10^{11}	1.47×10^{13}	2.70	2.05	95.25

Table 5 Physico chemical properties of pre-filtered sweet orange juice and microfiltered juice at 206.94 kPa transmembrane pressure

Property	Pre-filtered juice	Permeate	Change (%)	Sum of squares		Mean sum of squares		F value	P value	Remarks
				Between the groups	Within the groups	Between the groups	Within the groups			
TSS (°Brix)	9.0±0.057 (0.033)	8.86±0.115 (0.066)	0.78	0.0067	0.0333	0.0066	0.0083	0.80	0.421	Non-significant
pH	4.0±0.1 (0.057)	4.0±0.1 (0.057)	0.00	0.015	0.04	0.0151	0.0101	1.50	0.287	Non-significant
Colour (%A_{420})	1.913±0.009 (0.005)	1.827±0.008 (0.004)	4.49	0.0113	0.0003	0.0113	7.27E-05	155.01	0.0002	Significant
Clarity (%T_{650})	3.8±0.057 (0.033)	5.0±0.1 (0.057)	30.54	2.0416	0.026667	2.0417	0.0067	306.20	6.26E-05	Significant
Density (kg m^{-3})	1034±5.567 (3.214)	1029±5.409 (2.603)	0.48	28.1667	102.667	28.1667	25.6667	1.09	0.354	Non-significant
Viscosity (mPa s)	4.52±0.104 (0.06)	1.32±0.01 (0.005)	70.79	15.424	0.021	15.424	0.0054	2821.47	7.52E-07	Significant
Vitamin C (mg/100 g)	35.74±0.13 (0.074)	35.70±0.14 (0.084)	0.11	0.0024	0.07593	0.0024	0.0189	0.12	0.740	Non-significant
Titrable acidity (%)	0.84±0.1 (0.005)	0.83±0.005 (0.003)	1.19	6.67E-05	0.000267	6.67E-05	6.67E-05	1.00	0.373	Non-significant

F_{table} : 7.708 @ 5% level; Values in parenthesis indicate standard error

Note: Change (%) = $\frac{Pre-filtered\ juice-Permeate}{Pre-filtered\ juice}$ x 100

3.7 Profile of permeate properties

The properties of pre-filtered juice and microfiltered juice were expressed as mean of triplicate runs and the standard errors were reported as the arithmetic standard deviation of the three replicates (Table 6). It was noticed that most of the TSS, pH and vitamin C expressed as ascorbic acid of the feed were regained in the permeate and there was no loss of the important properties pertaining to sweet orange juice during filtration implying that the sugars and acid permeate through the pores of the membrane freely. Non significant reduction of total TSS in permeate was observed. Further, the viscosity of feed (4.52±0.104 mPa.s) was significantly reduced in permeate stream (1.32±0.01 mPa.s) due to retention of juice sacs with high molecular weight compounds like insoluble proteins, pectin, phosphatides that are suspended on the membrane surface, allowing clear juice to pass through the membrane surface. Thus viscosity of the permeate is just above pure water at room temperature (0.81 mPa.S). A little improvement in the clarity (in terms of $\%T_{650}$) and colour ($\%A_{420}$) were observed. The mean values of colour, clarity, viscosity of feed and permeate were significantly differed at 5% level as calculated F statistic value was more than F_{table} value at specified degrees of freedom. The change in the density of juice in feed (1034±5.567 kg m^{-3}) and permeate (1029±5.409 kg m^{-3}) was not statistically significant as insoluble low methoxy gel with etherification of calcium ions with pectin was retained on the MF membrane surface clearly removing haze causing materials from the permeate. Similar results on improvement in clarity, reduction in viscosity and non-significant change in density, a little reduction in TSS were reported on microfiltration of kiwi juice using 0.3 micron pore diameter membrane (Qin et al., 2015). Similar results on recovery of TSS and acids during MF in permeate and improvement in clarity and were reported by Domingues et al. (2014) for passion fruit, Kazemi et al. (2013), Pagliero et al. (2011) for orange juice, Razi et al. (2011) for tomato juice, Rai et al. (2010) for watermelon juice and Habibi et al. (2011) for carrot juice.

4 Conclusion

Clarification of sweet orange juice by 0.2 μm cellulose acetate MF membrane in a batch stirred cell. A positive correlation between TMP and permeate flux was observed. Flux was majorly dictated by intermediate pore blocking in combination with growth of low methoxy gel layer on the membrane surface. The total and reversible resistances had significant increase as Δp increased whereas irreversible resistance was almost constant. Reversible resistance was considered as domineering resistance and 90% original permeate flux was recovered by following proper washing protocol to clean the cellulose acetate 0.2 μm pore size MF membranes. Permeate profile indicated that the most of the TSS, pH and ascorbic acid of the feed were retained in the clarified permeate and there was no loss of the important properties pertaining to sweet orange juice. Further, the viscosity of feed was significantly reduced in permeate stream. A little improvement in clarity (in terms of $\%T_{650}$) and colour ($\%A_{420}$) were observed.

Conflict of interest

Authors declare there is no conflict of interest.

References

Amador, J. R. 2011. Laboratory manual procedures for analysis of citrus products. In *Manual No. 054R10020.000-6*, 8-17. USA: John Bean Technologies Corporation, Inc.

Bagci, P. O. 2014. Effective clarification of pomegranate juice: A comparative study of pretreatment methods and their influence on ultrafiltration flux. *Journal of Food Engineering*, 141: 58–64.

Brião, V. B., and C. R. G. Tavares. 2012. Pore blocking mechanism for the recovery of milk solids from dairy wastewater by ultrafiltration. *Brazilian Journal of Chemical Engineering*, 29(02): 393-407.

Buslig, B. S., and R. D. Carter. 1974. Particle size distribution in orange juices. *Florida State Horticultural Society*, 302-306.

Carneiro, L., I. S. Sa, F. S. Gomes, V. M. Matta, and L. M. C. Cabral. 2002. Cold sterilization and clarification of pineapple juice by tangential microfiltration. *Desalination*, 148(1-3): 93-98.

Cassano, A., F. Tasselli, C. Conidi, and E. Drioli. Ultrafiltration of clementine mandarin juice by hollow fibre membranes. *Desalinination*, 241(1-3): 302-308.

Chhaya, R., G. C. Majumdar, and S. De. 2013. Primary clarification of stevia extract: A comparison between centrifugation and microfiltration. *Separation Science and Technology*, 48(1): 113–121.

Chilukuri, V. V. S., A. D. Marshall, P. A. Munro, and H. Singh. 2001. Effect of sodium dodecyl sulphate and cross-flow velocity on membrane fouling during cross-flow microfiltration of lactoferrin solutions. *Chemical Engineering and Processing*, 40(4): 321-328

Corrideg, M., W. Kerr, and L. Wicker. 2001. Particle size distribution of orange juice cloud after addition of sensitized pectin. *Journal of Agricultural and Food Chemistry* ,49(5): 2523−2526.

Domingues, R. C. C., A. A. Ramos, V. L. Cardoso, and M. H. M. Reis. 2014. Microfiltration of passion fruit juice using hollow fibre membranes and evaluation of fouling mechanisms. *Journal of Food Engineering*, 121(1): 73-79.

Field, R. W., D. Wu, J. A. Howell, and B. B. Gupta. 1995. Critical flux concept for microfiltration fouling. *Journal of Membrane Science*, 100(3): 259-272.

Habibi, A., A. Aroujalian, A. Raisi, and F. Zokaee. 2011. Influence of operating parameters on clarification of carrot juice by microfiltration process. *Journal of Food Process Engineering*, 34(3): 860-877.

Hérmia, J. 1982. Constant pressure blocking filtration laws: applications to power-law non-Newtonian fluids. *Transactions of the Institution of Chemical Engineers*, 60(3): 183-187.

Hoagland, P. D., G. Konja, E. Clauss, and M. L. Fisherman. 1997. HPSEC with component analysis of citrus and apple pectins after hollow fiber ultrafiltration. *Journal of Food Science*, 62(1): 69-74.

Kale, S., and P. G. Adsule. 1995. Citrus. In *Handbook of Fruit Science and Technology Production, Composition, Storage and Processing*, eds. D. K. Salunkhe, and S. S. Kadam, 47. Marcel Dekker Inc.

Kazemi, M. A., M. Soltanieh, M. Yazdanshens, and L. Fillaudeu. 2013. Influence of crossflow microfiltration on ceramic membrane fouling and beer quality. *Desalinization and Water Treatment*, 53(22-24): 4302-4312.

Kirk, D. E., M. W. Montgomery, and M. G. Kortekaas. 1983. Clarification of pear juice by hollow fiber ultrafiltration. *Journal of Food Science*. 48(6): 1663-1666.

Kotsanopoulos, K. V., and I. S. Arvanitoyannis. 2015. Membrane processing technology in the food industry: food processing, wastewater treatment, and effects on physical, microbiological, organoleptic, and nutritional properties of foods. *Critical Reviews in Food Science and Nutrition*, 55(9): 1147-1175.

Kyo-Jen, H., C. Yung-Hsiung, and T. Kuo-Lun. 2003. Modeling of cross-flow microfiltration of fine particle/macromolecule binary suspension. *Journal of Chemical Engineering of Japan*, 36(12): 1488-1497.

Lei, Q., M. Zhang, and L. Shen. 2016. A novel insight into membrane fouling mechanism regarding gel layer filtration: Flory-Huggins based filtration mechanism. *Scientific Reports*, 6: 333-343.

Machado, R. M. D., R. N., Haneda, B. P. Trevisan, and S. R. Fontes. 2012. Effect of enzymatic treatment on the cross-flow microfiltration of açaí pulp: Analysis of the fouling and recovery of phytochemicals. *Journal of Food Engineering*, 113(3): 442– 452

Mirsaeedghazi, H., S. M. Mousavi, Z. Emam-Djomeh, K. Rezaei, A. Aroujalian, and M. Navidbakhsh. 2011. Comparison between ultrafiltration and microfiltration in the clarification of pomegranate juice. *Journal of Food Process Engineering*, 35(3):424-436.

Nakamura, K., and K. Matsumoto. 2013. Separation properties of wastewater containing o/w emulsion using ceramic microfiltration/ultrafiltration (MF/UF) membranes. *Membranes*, 3(2): 87-97.

Nandi, B. K., B. D. Nakamur, and R. Uppaluri. 2012. Clarification of orange juice using ceramic membrane and evaluation of fouling mechanism. *Journal of Food Process Engineering*, 35(3): 403-423.

Oers, O. W. V., M. A. G. Vorstman, W. G. H. M. Muijseleer, and P. J. A. M. Kerkhof. 1992. Unsteady state flux decline behaviour in relation to presence of gel layer. *Journal of Membrane Science*, 73(2-3): 231-246.

Oliveira, R. C., R. C. Doce, and S. T. D. Barros. 2012. Clarification of passion fruit juice by microfiltration: analyses of operating parameters, study of membrane fouling and juice quality. *Journal of Food Engineering*, 111(2): 432-439.

Pagliero, C. N. A. Ochoa, and J. Marchese, 2011. Orange juice clarification by microfiltration: effect of operational variables on membrane fouling. *Latin American Applied*

Research, 41(3): 279-284.

Philip, G. C., and K. C. Davis. 1992. Process for making high brix citrus concentrate. Patent WO NO. 1992021253 A1.

Qin, G., X. Lu, W. Wei, J. Li, R. Cui, and S. Hu. 2015. Microfiltration of kiwifruit juice and fouling mechanism using fly-ash-based ceramic membranes. *Food and Bioproducts Processing*, 96(2): 278–284.

Ranganna, S. 2010. Proximate constituents (chap 1), Vitamins (chap 5). In *Handbook of Analysis and Quality Control for Fruit and Vegetable Products*, 9-16, 105-106. Mc Graw Hill

Rai, P., G. C. Majumdar, S. Dasgupta, and S. De. 2005. Quantification of flux decline of depectinized mosambi (Citrus sinensis [L.] Osbeck) juice using unstirred batch ultrafiltration. *Journal of Food Process Engineering*, 28(4): 359-377.

Rai, P., G. C. Majumdar, V. K. Jayanti, S. Dasgupta, and S. De. 2006. Alternative pretreatment methods to enzymatic treatment for clarification of mosambi juice using ultrafiltration. *Journal of Food Process Engineering*, 29(2): 202–218.

Rai, C., P. Rai, G. C. Majumdar, S. De, and S. Dasgupta. 2010. Mechanism of permeate flux decline during microfiltration of watermelon (*Citrullus lanatus*) Juice. *Food Bioprocess Technology*, 3(4): 545-553.

Razi, B., A. Aroujalian, A. Raisi, and M. Fathizadeh. 2011. Clarification of tomato juice by cross-flow microfiltration. *International Journal of Food Science and Technology*, 46(1):138-145.

Sagu, S. T., S. Karmakar, J. N. Emmanuel, and S. De. 2014. Primary clarification of banana juice extract by centrifugation and microfiltration. *Separation Science and Technology*, 49(8): 1156-1169.

Shahnawaz, M., S. A. Sheikh, and S. Minhas. 2013. Role of sodium benzoate as a chemical preservative in extending the shelf life of orange juice. *Global Advanced Research Journal of Food Science and Technology*, 2(1): 007-018.

Stryer, L. 1998. *Biochemistry*. New York: Freeman.

Syed, H. M., P. U. Ghatge, G. Machewad, and S. Pawar. 2012. Studies on preparation of squash from sweet orange. *Open Access Scientific Reports*, 1: 311.

Wolkoff, D. B., S. M. Pontes, A. L. Furtado, L. C. Cabral, R. H. Moretti, and V. M. Matta. 2004. Process development for obtaining a clarified sport drink from natural juices. In *International Conference Enginnering and Food*, 1-5. Held during Jan 1st , 2004 at Montpellier, France..

Wu, J. J. 2021. Improving membrane filtration performance through time series analysis. *Discover Chemical Engineering*, 7(1): page.

Youn, K. S., J. H. Hong, D. H. Bae, S. J. Kim, and S. D. Kim. 2004. Effective clarifying process of reconstituted apple juice using membrane filtration with filter-aid pre-treatment. *Journal of Membrane Science*, 228(2): 179-186.

Zaidi, S. K., and A. Kumar. 2005. Experimental analysis of a gel layer in dead-end ultrafiltration of a silica suspension. *Desalination*, 172(2): 107-117.